MAJOR ARTICLE

Fatal Neurological Respiratory Insufficiency Is Common Among Viral Encephalitides

Hong Wang,[1] Venkatraman Siddharthan,[1] Kyle K. Kesler,[1] Jeffery O. Hall,[2] Neil E. Motter,[1] Justin G. Julander,[1] and John D. Morrey[1]

[1]Institute for Antiviral Research and [2]Utah Veterinary Diagnostic Laboratory, Department of Animal, Dairy, and Veterinary Sciences, Utah State University, Logan

Background. Neurological respiratory insufficiency strongly correlates with mortality among rodents infected with West Nile virus (WNV), which suggests that this is a primary mechanism of death in rodents and possibly fatal West Nile neurological disease in human patients.

Methods. To explore the possibility that neurological respiratory insufficiency is a broad mechanism of death in cases of viral encephalitis, plethysmography was evaluated in mice infected with 3 flaviviruses and 2 alphaviruses. Pathology was investigated by challenging the diaphragm, using electromyography with hypercapnia and optogenetic photoactivation.

Results. Among infections due to all but 1 alphavirus, death was strongly associated with a suppressed minute volume. Virally infected mice with a very low minute volume did not neurologically respond to hypercapnia or optogenetic photoactivation of the C4 cervical cord. Neurons with the orexin 1 receptor protein in the ventral C3–5 cervical cord were statistically diminished in WNV-infected mice with a low minute volume as compared to WNV-infected or sham-infected mice without respiratory insufficiency. Also, WNV-infected cells were adjacent to neurons with respiratory functions in the medulla.

Conclusions. Detection of a common neurological mechanism of death among viral encephalitides creates opportunities to create broad-spectrum therapies that target relevant neurological cells in patients with types of viral encephalitis that have not been treatable in the past.

Keywords. West Nile virus; electromyography; optogenetic; flavivirus; alphavirus; neurons; encephalitis; respiratory.

The precise mechanism of death among encephalitides caused by RNA viruses is largely unknown and has not been experimentally determined in animal models. For example, severe abnormal electrical activity or seizures in vital areas of the brain could presumably be fatal, as with Japanese encephalitis in children [1]. Vasculitis, damage to the capillary endothelial cells, can cause brain hemorrhaging, such as that due to eastern equine encephalitis virus [2]. Viruses could cause vasogenic breakdown of the blood-brain barrier or possibly cytotoxic edema associated with failure of ion homeostasis, with damage to the sodium/potassium pumps in glial cells [3]. Another possible cause of death is failure in autonomic function, but dysfunction is seldom the sole mechanism of death [4]. Specific damage to areas of the central nervous system controlling vital organ function might result in fatal organ failure [5]. Viral encephalitides may cause an array of these pathophysiological events, but any one of these events may be the physiological mechanism of death.

Also necessary for understanding viral encephalitic death is investigation of the mechanisms of cellular death in cell culture model systems, such as those involving induction of apoptosis by West Nile virus (WNV) capsid protein [6] or glutamate excitotoxicity contributing to neuronal death during Japanese encephalitis virus (JEV) infection [7]. Knowledge of the

Received 31 December 2012; accepted 6 February 2013; electronically published 2 May 2013.

Correspondence: John D. Morrey, PhD, 4700 Old Main Hill, Utah State University, Logan, UT 84322-4700 (john.morrey@usu.edu).

The Journal of Infectious Diseases 2013;208:573–83

DOI: 10.1093/infdis/jit186

cellular mechanism of death may not provide evidence about the physiological mechanism of death. Identification of the physiological mechanism of death for a particular viral encephalitis requires an experimental reductionist approach, hopefully with the use of appropriate animal models.

In this and prior studies, we have used neurophysiological approaches to investigate the pathophysiological events of West Nile neurological disease in rodent models. In a hamster model, it was determined that WNV infection of cholinergic motor neurons in the lumbosacral spinal cord impairs electrophysiological function of the neurons, reduces the number of functional motor units in the hind limbs, and results in paralysis [8]. Another study [9] demonstrated that electromyographic (EMG) activities in the diaphragm in WNV-infected hamsters were significantly ($P \leq .001$) less than EMG activities in sham-infected animals. When virus was stereotaxically injected directly into the ventrolateral medulla, suppression of EMG activities was especially rapid and robust. These data were the basis for another study in which abnormal plethysmographic parameters, such as diminished minute volume (MV), correlated strongly with mortality in mice and hamsters [10], whereas, no other disease outcomes correlated with mortality. These data are the basis for the hypothesis that respiratory insufficiency strongly contributes to mortality and may be the mechanism of death during WNV infection [10]. In this study, we investigated the possibility that respiratory insufficiency is also associated with mortality among mice infected with other flaviviruses and alphaviruses.

MATERIALS AND METHODS

Animals and Viruses

This work was done in the Association for Assessment and Accreditation of Laboratory Animal Care International–accredited laboratory of Utah State University and accorded with the National Institutes of Health Guide for the Care and Use of Laboratory Animals. Adult female BALB/c mice (age, >6 weeks; Charles River Laboratories) were used for infection with North American tick-borne encephalitis Powassan virus (POWV) [11], female CD-1 mice (age, >7 weeks) were used for infection with JEV, and female C57BL/6 mice (age, >7 weeks) were used for infection with WNV and neuroadapted Sindbis virus (NSV) [12]. Animals were randomly assigned to treatment groups by blindly selecting animals from a common container. WNV (5×10^4 plaque-forming units) and western equine encephalitis virus (WEEV; 80 median cell culture infectious doses [$CCID_{50}$]) were injected subcutaneously into the groin at a volume of 100 μL [9, 13, 14]. JEV (1.7×10^4 plaque-forming units) and POWV (6×10^3 $CCID_{50}$) were injected intraperitoneally at a volume of 100 μL. NSV (10^3 $CCID_{50}$) was injected intracranially at a volume of 20 μL. The WNV isolate (strain WN02), designated Kern 515, was recovered from a mosquito on 10 May 2007 in Kern County, California (TVP 10799 BBRC lot no. WNVKERN515-01, University of Texas Medical Branch Arbovirus Reference Collection). The WEEV isolate was obtained from the ATCC (no. VR-27). The JEV isolate, designated SA14, was obtained from BEI Resources (no. NR-2335). POWV isolate (strain M794), designated LB, was obtained from the University of Texas Medical Branch Arbovirus Reference Collection. NSV was obtained from Diane Griffin, Johns Hopkins Bloomberg School of Public Health. The virus titers in tissues were assayed using an infectious cell culture assay [15].

Transgenic mice [16] expressing channelrhodopsin from the choline acetyltransferase promoter (ChAT-mhChR2-YFP, Jackson Laboratories, catalog no. 014546) were used for optogenetic studies.

Rodents were judged as moribund if they did not step forward if prodded or if they did not right themselves when placed on their backs, because this was the only predictive sign of WNV-associated mortality.

Plethysmography

Unrestrained whole-body plethysmography was performed as described elsewhere [10]. Mouse-sized plethysmograph chambers were used (emka Technologies, catalogue no. PLY 3213). The differential pressure was acquired by an acquisition amplifier at 1 kHz (USB ACQ 4, emka Technologies) and processed in analysis software (IOX Base 2c, IOX 1 PULMO 2c, emka Technologies). The resulting minute volumes (MVs) were plotted using Prism 5 (GraphPad Software).

Orexin 1 Receptor (Ox1R), Somatostatin, and Paired-like Homeobox 2b (Phox2b) Immunohistochemical Staining

For Ox1R and WNV counterstaining, adult C57BL/6 mice were infected with WNV and then monitored for MVs of >1 SD above the normal mean value (ie, >230 mL/min) or ≥3 SDs below the normal mean value (ie, ≤73 mL/min). Groups were sham-infected mice and WNV-infected mice with MVs of >1 SD above the normal mean value and WNV-infected mice with MVs of ≥3 SDs below the normal mean value. Cryostat coronal cervical cord (C3–5) sections (thickness, 10 μm) from paraformaldehyde-perfused mice were obtained, with every third section retained for examination. The sections were stained with human monoclonal antibody of WNV (MGAWN1, MacroGenics, Rockville, MD; 1:1000 dilution) and rabbit anti-Ox1R antibody (Millipore; 1:400 dilution). Secondary antibodies were Alexa Fluor 568 goat anti-human and Alexa Fluor 488 rabbit anti-mouse immunoglobulin G. Immunostaining procedures are described elsewhere [17]. Under a 20× objective lens, the number of neurons that stained positive for Ox1R was counted in ventral horn of each section, and the average number of positive cells per section was reported.

For Phox2b and WNV counterstaining, the retrotrapezoid nucleus (RTN) was located ventral to the facial nucleus and

juxtafacial lateral paragigantocellular [18]. Caudal medullary coronal sections (thickness, 10 μm) extending about 0.3 mm from the front boundary of the cerebellum (ie, from Bregma −5.68 to −6.00 mm) were obtained [19]. Primary antibody of rabbit anti-Phox2b (Pierce Biotechnology, Rockford, IL; 1:400 dilution) and 7H2 mouse monoclonal antibody for WNV envelope protein (BioReliance, Rockville, MD; 1:460 dilution) were used [20].

For somatostatin staining, paraffin sections (thickness, 5 μm) were processed [21] and incubated with the humanized monoclonal antibody MGAWN1 and the polyclonal anti-somatostatin antibody (Immunostar, Hudson, WI). Alexa Fluor fluorescent secondary antibodies (Molecular Probes, Eugene, OR) were used. We verified the specificity of the anti-somatostatin antibody on the basis of characteristic staining of islets of Langerhans cells [22].

Optogenetic Photoactivation of Phrenic Motor Neurons

Transgenic mice [16] (Jackson Laboratories, catalog no. 014546) expressing channelrhodopsin from the ChAT promoter were infected and then monitored with plethysmography for suppression of EMG activity to >2 SDs below the normal mean value (ie, 112 mL/min for C57BL/6 mice; n = 1315). Animals with MV suppression to >2 SDs below the normal mean value were anesthetized with ketamine/xylazine, and the optical fiber was surgically implanted. The exposure of dorsal vertebra of the cervical cord was performed on a stereotaxic apparatus [9]. An optical fiber (Thorlabs) with a 200-μm diameter was implanted to a depth of 1 mm–0.5 mm at a location midlateral to the right semi–cervical cord, between C4 and C5. The fiber was secured with dental cement.

Evaluation of EMG activity in the diaphragm was based on procedures previously described elsewhere [9, 23, 24]. A pair of 40-gauge Teflon-insulated single-stranded stainless steel wires (AS765-40 Cooner Wire, Specialty Wire and Cable) was implanted in the midcostal region of the right hemidiaphragm. A common ground wire was implanted subcutaneously. Leads were connected to a differential DAM50 amplifier (World Precision Instruments) set at a 10 K gain with a band-pass filter between 300 Hz and 3 kHz. EMG recordings were monitored by a digital storage oscilloscope.

For surgical bilateral vagotomy and ventilation, both vagus nerves identified in the carotid sheath were cut distally to the carotid bifurcation to abolish mechanoreceptor feedback and entrainment. Tracheostomy was performed in the midline of the neck, and a tracheal cannula connected to an artificial ventilator (50 cycles/min; Harvard Apparatus) was inserted into the trachea [25, 26].

Bilateral vagotomized and mechanically ventilated mice were subjected to photoactivation using a 470-nm blue laser (Opto Engine, Midvale, UT). A 12-mW laser pulse was delivered by the laser via the optical fiber at 20 Hz with a 40% duty cycle [27]. The output power and pulse timing of the laser were verified using a 470-nm power meter (Opto Engine) and a digital storage oscilloscope (2542BK BK Precision Electronic Test Instruments, Yorba Linda, CA), respectively. The pulse was delivered in 500-ms on/off trains, using in-house Labview programming (National Instruments, Austin, TX), to allow time for the diaphragm to relax between simulations. The root mean square of the EMG activity in the diaphragm was recorded and used for comparison. The resulting waveforms were graphed in Prism 5 (GraphPad Software).

Hypercapnia Challenge

C57BL/6 and BALB/c mice were infected with the respective viruses and then monitored with plethysmography for suppression of the MV to >2 SDs below the normal mean value. Animals with MV suppression to >2 SDs below the normal mean value were anesthetized, and the EMG activity in the diaphragm was recorded. Following the baseline recording, bilateral vagotomies and intubations for mechanical ventilation were performed. Another diaphragm recording was obtained while under the influence of mechanical ventilation, following the vagotomy. The CO_2 content of the expired breath was recorded using an in-line capnograph (K-33 ICB CO_2 Sensor, CO_2 Meter, Ormond Beach, FL) and processed in CO_2 DAS software. The mice were then gradually exposed to increasing levels of CO_2, using an air-CO_2 gas mixture (maximum proportions, 7% CO_2, 21% O_2, and 72% N). EMG activity in the diaphragm in response to hypercapnia gas was recorded at 1 kHz on a digital storage oscilloscope. The root mean squares of the EMG waveforms were calculated.

RESULTS

To determine the prevalence of respiratory insufficiency among viral encephalitides, plethysmography was monitored over the course of disease in mice infected with WNV, JEV, NSV, POWV, or WEEV (Figure 1). As determined previously, respiratory insufficiency, identified on the basis of reduction of the MV to >2 SDs below the normal mean value, was strongly associated with death of WNV-infected mice. This was also true for mice infected with JEV or NSV. The association was not as strong in mice infected with POWV. Respiratory insufficiency was not associated with the death of mice infected with WEEV.

Viral titers of brain tissue ($P \leq .01$) and spinal cord tissue ($P \leq .05$) from WNV-infected animals with MVs of >2 SDs above the normal mean value were significantly less than titers for animals with abnormal MVs of >2 SDs below the normal mean value (Figure 2). These findings appeared to be similar to those for brain and spinal cord tissues of mice infected with NSV and POWV, but the differences were not statistically different, possibly because of smaller sample sizes. Respiratory insufficiency was likely due to neurological deficits rather than

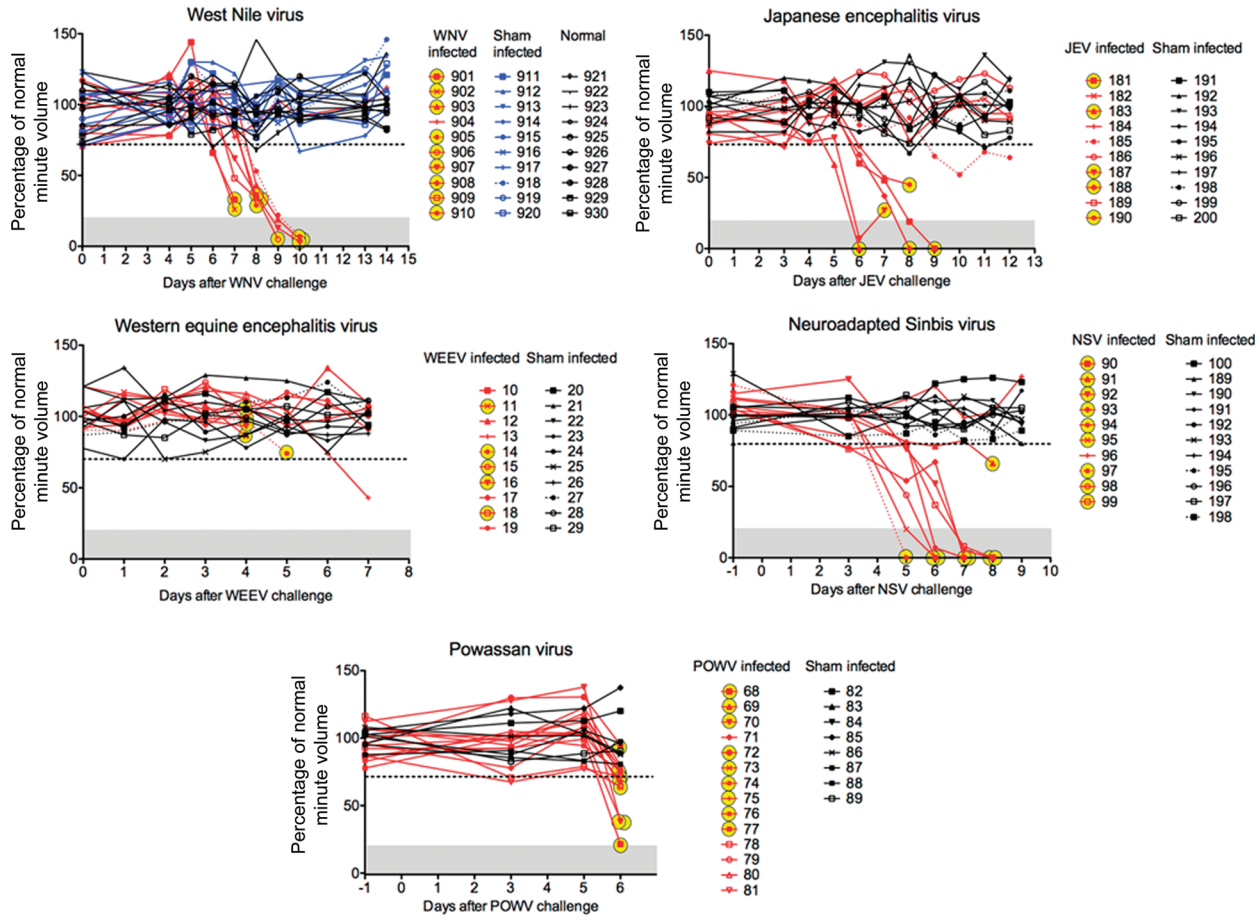

Figure 1. Association of mortality with suppressed minute volume in mice infected with West Nile virus (WNV), Japanese encephalitis virus (JEV), neuroadapted Sindbis virus (NSV), Powassan virus (POWV), and western equine encephalitis virus (WEEV). To calculate the daily normal mean minute volume (MV) for determining the percentage of the normal mean value for each measurement, 10 normal mice for WNV, 10 sham-infected mice for JEV, 10 sham-infected mice for NSV, 8 sham-infected mice for POWV, and 10 sham-infected mice for WEEV were used. The horizontal dotted lines were 2 SDs from the normal mean values across all days.

to extraneurological respiratory disease, because no abnormal histopathological findings were observed in the lungs and diaphragms of infected mice with reduced MVs. All mice with respiratory insufficiency infected with NSV or POWV (4 mice in each group) did not have histopathological lesions in their diaphragms or lungs, whereas all animals had lesions in their spinal cords and brains (data not shown). Viral titers in the central nervous system and the lack of abnormal histopathological findings in the lungs or diaphragms are consistent with neurological disease rather than extraneurological respiratory disease.

To investigate neurological respiratory function, virally infected mice were ventilated, intubated, challenged with hypercapnia (7% CO_2), and monitored for EMG activity in the diaphragm (Figure 3). As predicted, the diaphragmatic EMG activities in sham-infected mice with normal MV were easily identified before ventilation and were not detectable after ventilation and vagotomy (Figure 3). These sham-infected mice responded to hypercapnia, as evidenced by detection of EMG activity in the diaphragm (Figure 3). The same analysis was performed with virus-infected mice with low MVs of >2 SDs below the normal mean value. The diaphragmatic EMG activities in 2 WNV-infected mice (mouse 577 and mouse 594) with low MVs (24 and 46 mL/min, respectively) did not respond to hypercapnia. Another WNV-infected mouse (mouse 596) did respond with diaphragmatic EMG activity, but the MV was much higher, at 108 mL/min, and just >2 SD below the normal mean value for C57BL/6 mice (112 mL/min). Similar results were obtained for mice infected with POWV and NSV. However, C57BL/6 mice infected with WEEV that had either low MVs (47 mL/min [mouse 392]) or high MVs (193 mL/min [mouse 307] and 196 mL/min [mouse 306]) had strongly detectable EMG activity in the diaphragm. In short, the diaphragms of mice infected with WNV, POWV, and NSV that had low MVs did not have a normal electrophysiological response to hypercapnia, whereas mice with fatal WEEV infection responded to hypercapnia.

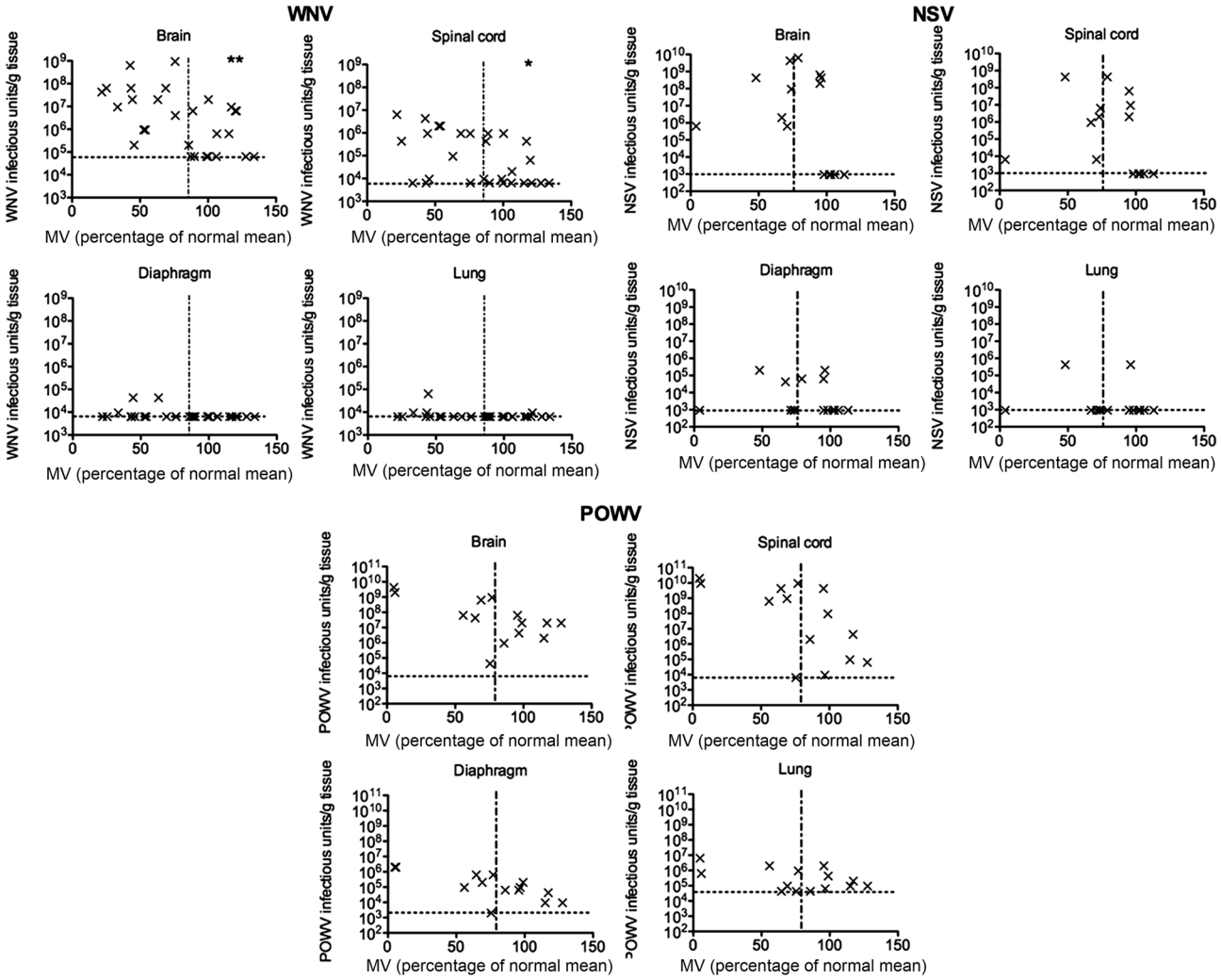

Figure 2. Association of viral titers with suppressed minute volume in mice infected with West Nile virus (WNV), neuroadapted Sindbis virus (NSV), and Powassan virus (POWV) in brain, spinal cord, diaphragm, and lung tissues. Viral infected mice were necropsied when the minute volume was >2 SDs below the normal mean value (vertical dotted lines). A corresponding mouse with an MV of >2 SDs above the normal mean value was also necropsied. Tissues were homogenized and processed for infectious virus titers. Percentages of the normal mean MVs were calculated as described in Figure 1. The horizontal lines were the limits of detection. $^{*}P \leq .05$ and $^{**}P \leq .01$, by the nonparametric Mann–Whitney 2-tailed test.

We probed the function of phrenic motor neurons innervating the diaphragm, using optogenetic photoactivation, in transgenic mice expressing channelrhodopsin from the ChAT promoter. WNV- and NSV-infected mice were monitored for MVs that were >2 SDs below the normal mean value. These virally infected and sham-infected mice were intubated and vagotomized, after which optical fibers were inserted into the C4 vertebrae, by means of laminectomy [20]. The EMGs activities in the diaphragms of sham-infected mice with normal MVs were directly aligned with the photoactivation signals (Figure 4). Diaphragms in 2 of 3 NSV-infected transgenic mice did not respond to photoactivation, as evidenced a lack of diaphragmatic EMG activity (ie, lower EMG readings). The diaphragmatic EMG activity in 1 NSV-infected mouse that responded to photoactivation (mouse 172) appeared to have hyperexcitability, which was probably caused by neuronal damage [28, 29]. The diaphragms from all 3 WNV-infected mice with MVs well below 2 SDs below the normal mean value did not respond to photoactivation of phrenic neurons (Figure 4).

To investigate the possibility that viral infection was damaging or destroying the ability of phrenic motor neurons to contribute to or cause respiratory failure, neurons were identified immunohistochemically by staining for Ox1R, because orexin, a neuropeptide originating from the hypothalamus, innervates phrenic neurons through Ox1R in the cervical cord [30, 31] (Figure 5). The number of Ox1R-positive neurons in the ventral horn of the C3–C5 cervical cord of WNV-infected mice with respiratory insufficiency were significantly lower than

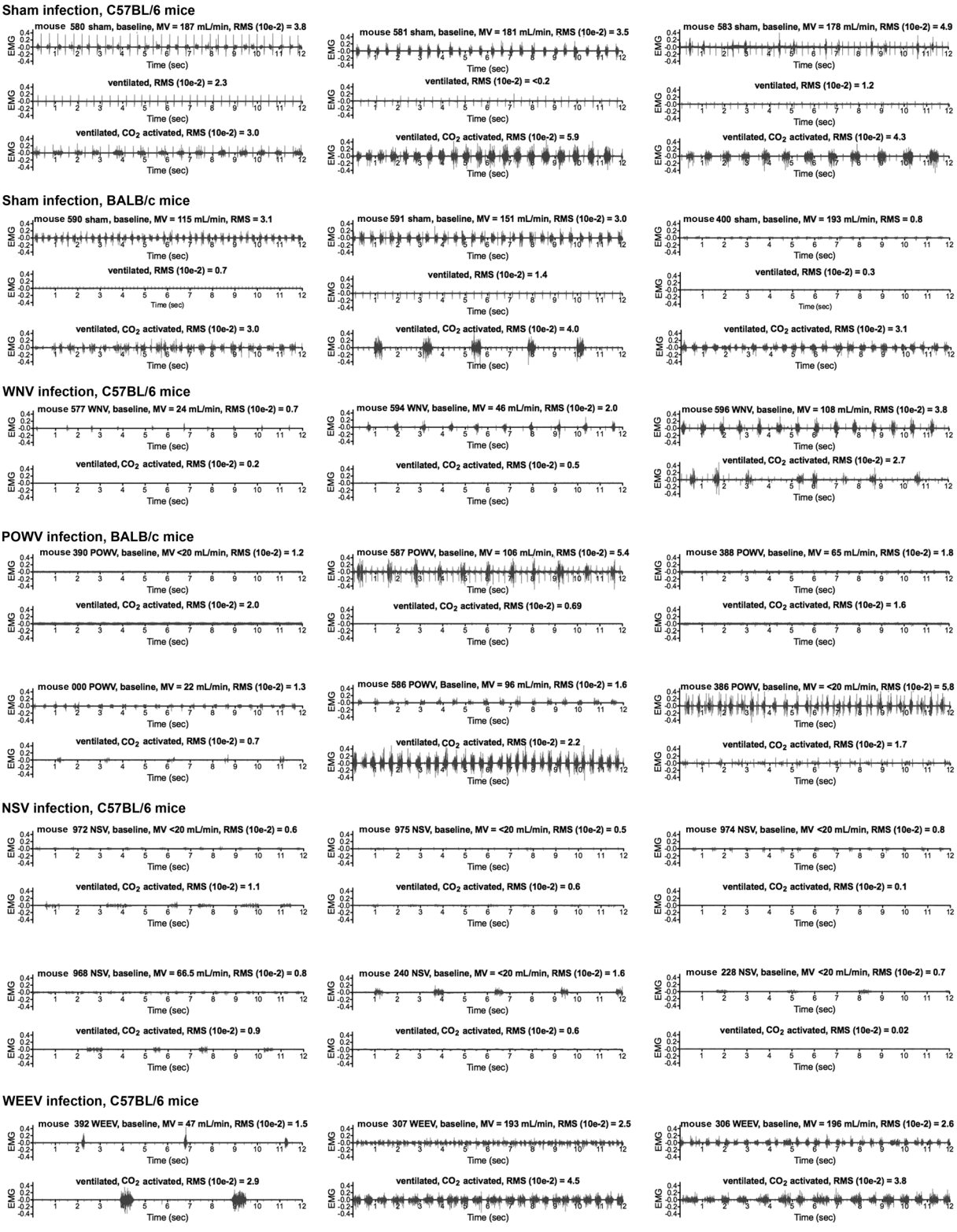

Figure 3. Effect of viral infections on diaphragmatic electromyographic (EMG) activities for mice challenged with hypercapnia. C57BL/6 and BALB/c mice underwent sham infection; C57BL/6 mice underwent West Nile virus (WNV), neuroadapted Sindbis virus (NSV), or western equine encephalitis virus (WEEV) infection; and BALB/c mice underwent Powassan virus (POWV) infection. Plethysmography was performed daily to detect the virally infected mice with minute volumes (MVs) of >2 SDs below the normal mean MVs, as calculated in Figure 1. The diaphragmatic EMG activities of these mice with respiratory insufficiencies were then measured in mice before (top EMG readings) and after intubation and vagotomy (middle EMG readings). The mice were challenged with 7% CO_2, and the diaphragm EMGs were measured (bottom EMG readings). Mouse identification numbers, MVs, and root mean squares (RMSs) reflecting the amplitudes are all listed above the EMG readings.

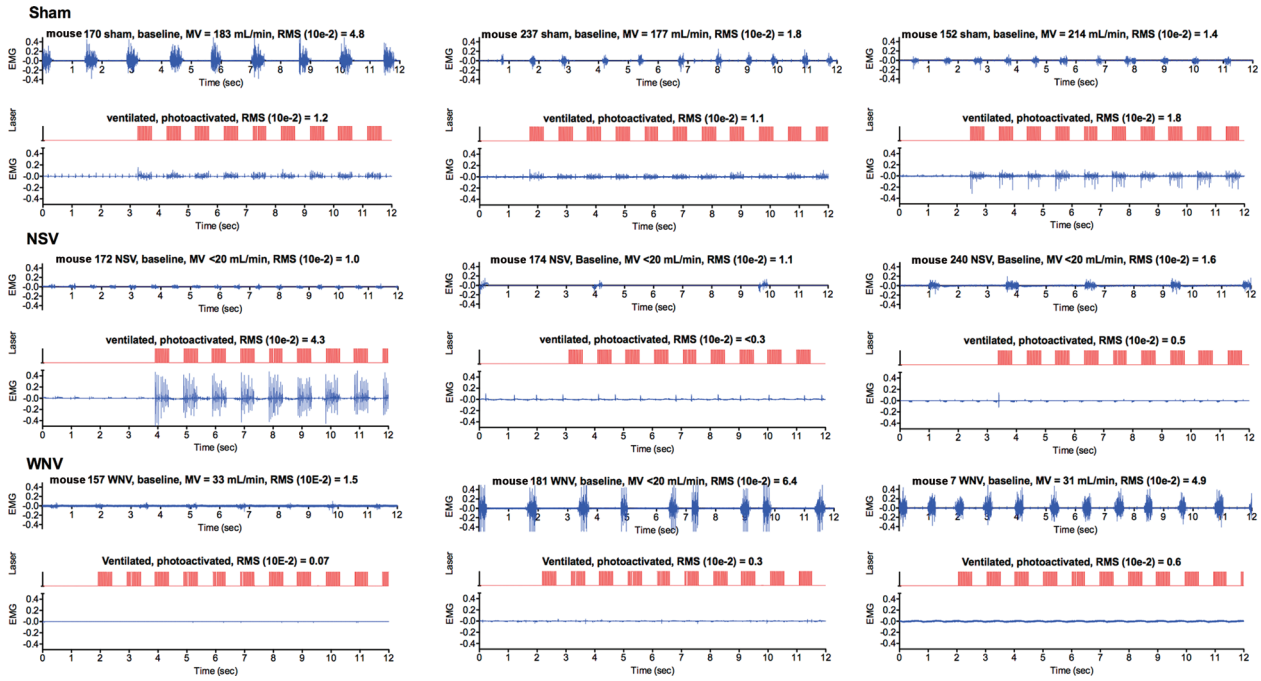

Figure 4. Effect of viral infections on electromyographic (EMG) activities in diaphragms of ChAT-mhChR2-YFP transgenic mice challenged with optogenetic photoactivation of C4 cervical cord containing motor neurons innervating the diaphragm. Mice underwent sham infection or were infected with neuroadapted Sindbis virus (NSV) or West Nile virus (WNV). Plethysmography was performed daily to detect the virally infected mice with MVs of >2 SDs below the normal mean MV, as calculated in Figure 1. The diaphragmatic EMG activities for these mice with respiratory insufficiencies were then measured in mice before (top EMG readings) and after intubation and vagotomy (data not shown) to confirm the absence of EMG readings. An optical fiber was inserted into the C4 vertebra by laminectomy [20]. Diaphragmatic EMG was used to measure photoactivation of the phrenic neurons. The EMG activities in the diaphragm (blue) were directly aligned with the photoactivation signals (red). Mouse identification numbers, MVs, and root mean squares (RMSs) reflecting the amplitudes are listed above the EMG readings.

those in the sham-infected mice ($P \leq .05$; Figure 5*A*). The number of Ox1R-positive neurons in WNV-infected mice with normal MVs was slightly less than that in sham-infected mice, but the difference was not statistically significant. For 2 of the 4 WNV-infected mice with normal MVs, the number of Ox1R-positive neurons was the same as that in mice with abnormal MVs, such that, given a couple of more days, the mice might have developed abnormal MVs. WNV envelope staining was detected in tissue sections from all 4 WNV-infected mice with reduced MVs (Figure 5*B*), whereas viral staining was observed in only 1 of 4 WNV-infected mice with normal MVs (data not shown).

To determine whether WNV could infect areas of the brainstem that are active in respiratory control, the ventral medullas of WNV-infected mice were stained for somatostatin neuropeptide, which has respiratory control functions [32], and for Phox2b, which regulates breathing in a CO_2-dependent manner in the RTN [26, 33]. WNV envelope staining was colocalized, with some somatostatin staining of neurons in focal areas of the brainstem (Figure 6*A*). Even though quantification was not performed, these data indicated that WNV could infect somatostatin-containing neurons. In the RTN, WNV-infected cells with the morphology of glial cells were identified adjacent to Phox2b-stained neurons (Figure 6*B*). Although we did not observe colocalization of WNV staining with Phox2b staining, the proximity of WNV-infected glial cells next to Phox2b-stained neurons in the RTN suggests that WNV infection might affect the chemoreceptor functions of neurons by secondary effects in the RTN.

DISCUSSION

This study addressed whether respiratory insufficiency was the probable physiological cause of death among mice with various viral encephalitides. As previously determined, respiratory insufficiency is strongly associated with mortality in rodents infected with WNV. No other disease outcomes correlate with mortality, including motor unit number estimations [8], brain auditory evoked response [9], blood-brain barrier permeability [14], and memory impairment [34]. The diaphragms or lungs of these animals do not have any abnormal pathological findings to account for mortality [9]. Moreover, respiratory distress in human patients is a serious outcome of West Nile neurological disease [35], which can result in respiratory failure

A

Sham infected Normal MV	WNV infected Normal MV	WNV infected Abnormal MV
18 ± 3.3	10 ± 3.1	5 ± 6.3
18 ± 2.6	21 ± 6.1	8 ± 10.7
23 ± 3.3	9 ± 2.5	13 ± 5.0
24 ± 4.1	24 ± 2.8	11 ± 4.6
21 ± 3.2	16 ± 7.6	9 ± 3.5*

B

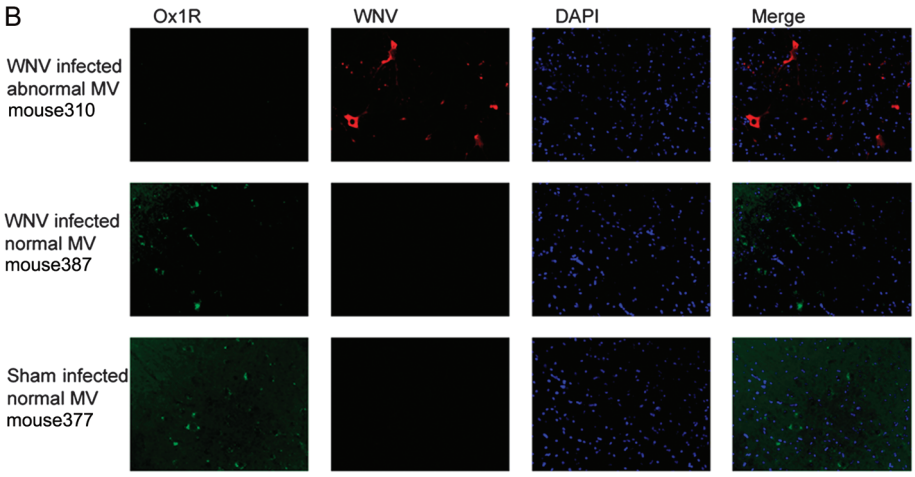

Figure 5. Orexin 1 receptor (Ox1R)–stained cells in the ventral horn of cervical cords (C3–C5) of West Nile virus (WNV)–infected mice with respiratory insufficiency. *A*, Quantification of Ox1R-stained cells, as measured by minute volume (MV), compared with controls. Each value represents a mean number (±SD) of positive cells per coronal section of the cervical cord. Every third section (12 μm) was collected, for a total of 40 sections per cervical cord. A normal MV was defined as an MV of >1 SD above the normal mean value (ie, 151 mL/min) from 1315 readings of C57BL/6 mice from prior experiments during the past half year. An abnormal MV was defined as an MV of >3 SDs below the normal mean value (ie, 73 mL/min). One-way analysis with the Newman-Keuls multiple comparison test (*$P < .05$, compared with the sham-infected group). *B*, Immunohistochemistry findings for 1 representative of 4 animals in each of 3 the groups (ie, mouse 310 from the group of WNV-infected mice with abnormal MVs, mouse 387 from the group of WNV-infected mice with normal MVs, and mouse 377 from the group of sham-infected mice with normal MVs). Mice were injected subcutaneously with either WNV or sham, and the MVs were monitored. Mice with abnormal MVs of >3 SDs below the normal mean value (ie, 73 mL/min) were euthanized for immunohistochemical staining of Ox1R and WNV envelope. For each WNV-infected mouse, another WNV-infected mouse with a normal MV of >1 SD above the normal mean value (ie, 151 mL/min) and a sham-infected mouse were selected for immunohistochemistry analysis.

with a poor prognosis [36]. In this study, 3 flaviviruses were investigated: WNV, JEV, and POWV. All 3 viruses are known to primarily infect neurons [37–41]. Two alphaviruses were also evaluated: WEEV and NSV. Like the flaviviruses studies, NSV primarily infects neurons [12], whereas Venezuelan equine encephalitis virus, which is closely related to WEEV, has a broader tropism that includes glial cells [42].

Remarkably, encephalitides due to all but one of the viruses (ie, WNV, JEV, POWV, and NSV, but not WEEV) that were evaluated by plethysmography revealed an association of respiratory insufficiency with mortality. The association was not as strong with POWV, however, possibly because the declining MV associated with POWV infection was more difficult to observe over time because of the abrupt and rapid onset of mortality; future studies of this association are therefore needed. Additionally, the diaphragmatic EMG activities were below or near the limits of detection in WNV-, POWV-, NSV-infected mice with suppressed plethysmography values, as measured by MVs. Even though WEEV extensively infects the central nervous system [43], fatality of WEEV-infected mice did not correlate with respiratory insufficiency, nor did the diaphragms lose their ability to respond to stimulation from hypercapnia or optogenetic photoactivation of cervical cord phrenic neurons. Future investigations of the neuropathological differences between encephalitides due to WEEV and those due to the other viruses investigated here should provide further insights about the mechanism of fatal respiratory insufficiency.

To clearly detect stimulation of the diaphragm by hypercapnia or photoactivation of the phrenic neurons, diaphragmatic EMG activities were measured in anesthetized, intubated, and vagotomized mice that provided flat-line readings. Extraneous cardiac tracings could be identified, but they did not obscure the EMG tracings. The diaphragmatic EMG tracings of all WNV-, POWV-, and NSV-infected mice with very low MVs were undetectable or nearly undetectable, whereas infected mice with MVs within 2 SDs of the normal mean value were identifiable. One exception was the EMG activity associated with photoactivation of mouse 172, which had an MV of <20 mL/min but a large amplitude of activity detected by EMG (Figure 4). We speculate that the neurons regulating diaphragmatic EMG activity in

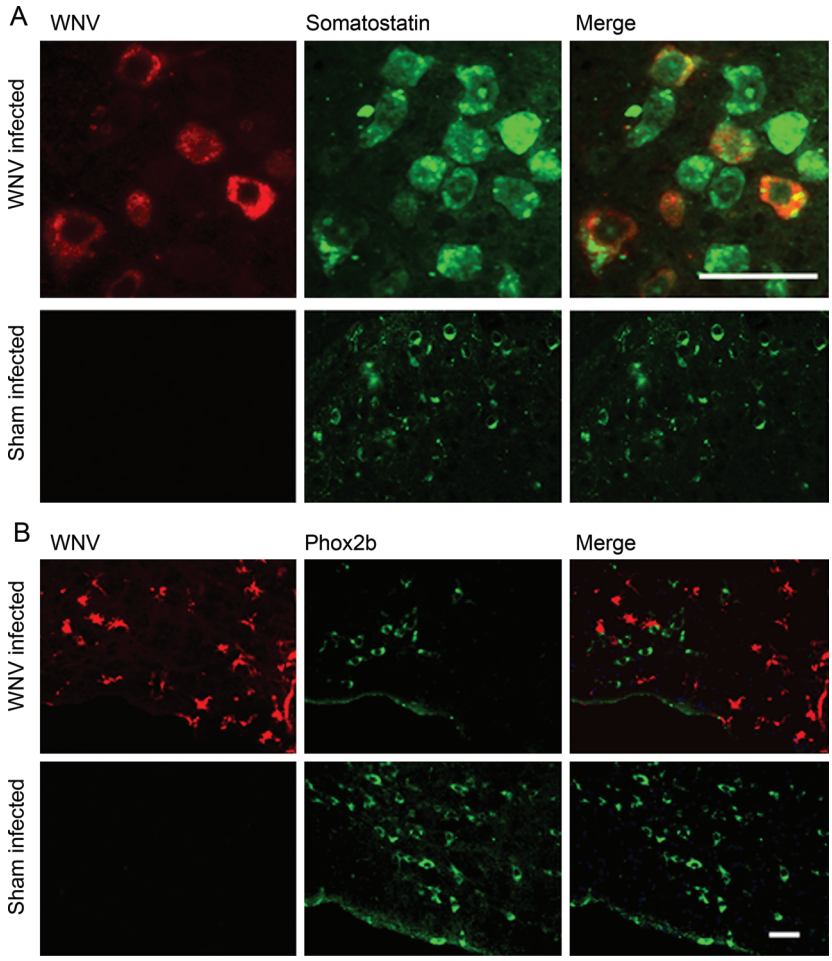

Figure 6. Somatostatin- and paired-like homeobox 2b (Phox2b)–stained cells in the medulla of West Nile virus (WNV)–infected mice. Examples of immunohistochemistry findings for WNV-infected mice with reduced minute volumes (MVs) as compared to sham-infected mice. *A*, Somatostatin and WNV staining. *B*, Phox2b and WNV staining. Separate mice were used in panels *A* and *B*. Scale bar, 50 μm.

this mouse may have experienced hyperexcitability before completely losing their function [28, 29].

The association of low diaphragmatic EMG activities with photoactivation of phrenic neurons was supported by the loss of Ox1R-positive phrenic neurons in WNV-infected mice with low MVs but not in infected- or sham-infected mice with normal MVs. The orexin neuropeptide originating from the hypothalamus is a ligand for Ox1R in phrenic neurons, but Ox1R is also present on other neurons in the cervical cord, so we were not certain that loss of Ox1R-positive neurons was a loss of phrenic neurons. Nevertheless, WNV does infect motor neurons throughout the spinal cord [20, 37], so it is reasonable to conclude that phrenic motor neurons were also lost.

The inability of virally infected mice with low MVs to respond to hypercapnia may be due to neuronal damage in the ventral medulla. In these studies, virally infected mice with low MVs did not respond to hypercapnia by stimulating the diaphragmatic EMG activities. This indicated that neuronal damage occurred from virus infection of neurons ranging from the chemoreceptor neurons in the ventral medulla to the phrenic neurons in the cervical cord. Theoretically, the lack of hypercapnia compensation may have solely been due to damaged phrenic neurons, but evidence from somatostatin and Phox2b staining suggests that damage to respiratory control neurons in the medulla may have contributed to the respiratory insufficiency. Since somatostatin neuropeptide in the medulla affects chemosensory drive [32], the observation that WNV can directly infect somatostatin-containing neurons indicated that this virus can infect at least this subset of respiratory control neurons in the medulla. The other evidence that WNV may affect respiratory functions in the ventral medulla was the presence of WNV-stained glial cells in the area of Phox2b-stained neurons that regulate breathing in a CO_2-dependent manner within the RTN [26, 33].

Knowledge of the physiological mechanisms for disease outcomes, including death, would allow researchers to focus on disease-relevant neurological tissues and cell types to investigate immunological, molecular, and cellular pathological

events. As examples of the importance of knowing the neurophysiological mechanism of disease, investigators focus on motor symptoms originating from the death of dopaminergic neurons in the substantia nigra for Parkinson disease [44]. For amyotropic lateral sclerosis, investigators focus on motor neurons in the ventral horn of the spinal cord and the cortical neurons that provide their efferent input [45]. Unfortunately, the neurophysiological reason for death from encephalitis caused by RNA viruses is largely unknown. Since the encephalitic viruses typically infect many anatomical areas of the central nervous system, which may or may not result in functional deficits, determining the mechanism of death is not straightforward and requires a reductionist approach, as used here. Future studies should include investigations of other encephalitic alphaviruses, including Venezuelan equine encephalitis virus and eastern equine encephalitis virus, in light of the observation that WEEV did not result in fatal respiratory insufficiency.

The unique contribution of this study is that fatal respiratory insufficiency is caused by large group of viruses other than WNV alone [10] and that damaged phrenic motor neurons in the cervical cord and possibly damaged respiratory control neurons in the ventral medulla lead to this respiratory insufficiency. This finding will allow investigators to focus on disease-relevant neurological tissues and cells to better improve the treatment and management of multiple viral encephalitides.

Notes

Acknowledgments. We thank Ashley Dagley (Utah State University), for expert technical assistance; David Poldiak (emka Technologies), Ronald M. Harper, (Department of Neurology, University of California at Los Angeles), and Patrice G. Guyenet (Department of Pharmacology, University of Virginia), for helpful suggestions; Ramona Skirpstunas (Diplomat of the American College of Veterinary Pathology), for histopathologic analysis; and Diane E. Griffin (Johns Hopkins Bloomberg School of Public Health), for providing NSV.

Financial support. The work was supported by the Rocky Mountain Regional Centers of Excellence, National Institute of Allergy and Infectious Diseases (NIAID), National Institutes of Health (NIH; grant U54 AI-065357 to J. D. M.); Virology Branch, NIAID, NIH (grant HHSN272201000039I to J. D. M.); and the Utah Agriculture Research Station (grant UTA00424 to J. D. M.).

Potential conflicts of interest. All authors: No reported conflicts.

All authors have submitted the ICMJE Form for Disclosure of Potential Conflicts of Interest. Conflicts that the editors consider relevant to the content of the manuscript have been disclosed.

References

1. Misra UK, Kalita J. Seizures in Japanese encephalitis. J Neurol Sci **2001**; 190:57–60.
2. Paessler S, Aguilar P, Anishchenko M, et al. The hamster as an animal model for eastern equine encephalitis—and its use in studies of virus entrance into the brain. J Infect Dis **2004**; 189:2072–6.
3. Kitchener N. Cerebral edema. In: Kitchener N, Hashem S, Wahba M, Khalaf M, Zarif B, Mansoor S, eds. Critical care in neurology. Flying Publisher, Wuppertal, Germany. **2012**:79–83.
4. Bannister R, Mathias CJ. Clinical features and evaluation of the primary chronic autonomic failure syndromes. In: Bannister R, Mathias CJ, eds. Autonomic failure: a textbook of clinical disorders of the autonomic nervous system. 4th ed. New York: Oxford University Press, **2004**:307–16.
5. Shindarov LM, Chumakov MP, Voroshilova MK, et al. Epidemiological, clinical, and pathomorphological characteristics of epidemic poliomyelitis-like disease caused by enterovirus 71. J Hyg Epidemiol Microbiol Immunol **1979**; 23:284–95.
6. Yang JS, Ramanathan MP, Muthumani K, et al. Induction of inflammation by West Nile virus capsid through the caspase-9 apoptotic pathway. Emerg Infect Dis **2002**; 8:1379–84.
7. Chen CJ, Ou YC, Chang CY, et al. Glutamate released by Japanese encephalitis virus-infected microglia involves TNF-alpha signaling and contributes to neuronal death. Glia **2012**; 60:487–501.
8. Siddharthan V, Wang H, Motter NE, et al. Persistent West Nile virus associated with a neurological sequela in hamsters identified by motor unit number estimation. J Virol **2009**; 83:4251–61.
9. Morrey JD, Siddharthan V, Wang H, et al. Neurological suppression of diaphragm electromyographs in hamsters infected with West Nile virus. J Neurovirol **2010**; 16:318–29.
10. Morrey JD, Siddharthan V, Wang H, Hall JO. Respiratory insufficiency correlated strongly with mortality of rodents infected with west nile virus. PLoS One **2012**; 7:e38672.
11. Ebel GD. Update on Powassan virus: emergence of a North American tick-borne flavivirus. Annu Rev Entomol **2010**; 55:95–110.
12. Jackson AC, Moench TR, Trapp BD, Griffin DE. Basis of neurovirulence in Sindbis virus encephalomyelitis of mice. Lab Invest **1988**; 58:503–9.
13. Morrey JD, Siddharthan V, Olsen AL, et al. Humanized monoclonal antibody against West Nile virus E protein administered after neuronal infection protects against lethal encephalitis in hamsters. J Infect Dis **2006**; 194:1300–08.
14. Morrey JD, Olsen AL, Siddharthan V, et al. Increased blood-brain barrier permeability is not a primary determinant for lethality of West Nile virus infection in rodents. J Gen Virol **2008**; 89:467–73.
15. Morrey JD, Smee DF, Sidwell RW, Tseng CK. Identification of active compounds against a New York isolate of West Nile virus. Antiviral Res **2002**; 55:107–16.
16. Zhao S, Ting JT, Atallah HE, et al. Cell type-specific channelrhodopsin-2 transgenic mice for optogenetic dissection of neural circuitry function. Nat Methods **2011**; 8:745–52.
17. Wang H, Siddharthan V, Hall JO, Morrey JD. Autonomic nervous dysfunction in hamsters infected with West Nile virus. PLoS ONE **2011**; 6: e19575.
18. Cream C, Li A, Nattie E. The retrotrapezoid nucleus (RTN): local cytoarchitecture and afferent connections. Respir Physiol Neurobiol **2002**; 130:121–37.
19. Paxinos G, Franklin KBJ. The mouse brain in stereotaxic coordinates: compact second edition. 2nd ed. Elseiver Science, Amsterdam, the Netherlands. **2004**.
20. Morrey JD, Siddharthan V, Wang H, et al. West Nile virus-induced acute flaccid paralysis is prevented by monoclonal antibody treatment when administered after infection of spinal cord neurons. J Neurovirol **2008**; 14:152–63.
21. Stornetta RL, Rosin DL, Wang H, Sevigny CP, Weston MC, Guyenet PG. A group of glutamatergic interneurons expressing high levels of both neurokinin-1 receptors and somatostatin identifies the region of the pre-Botzinger complex. J Comp Neurol **2003**; 455: 499–512.
22. Romero-Zerbo SY, Rafacho A, Diaz-Arteaga A, et al. A role for the putative cannabinoid receptor GPR55 in the islets of Langerhans. J Endocrinol **2011**; 211:177–85.
23. Campbell C, Weinger MB, Quinn M. Alterations in diaphragm EMG activity during opiate-induced respiratory depression. Respiration physiology **1995**; 100:107–17.
24. Fournier M, Lewis MI. Functional, cellular, and biochemical adaptations to elastase-induced emphysema in hamster medial scalene. J Appl Physiol **2000**; 88:1327–37.

25. Alilain WJ, Horn KP, Hu H, Dick TE, Silver J. Functional regeneration of respiratory pathways after spinal cord injury. Nature **2011**; 475: 196–200.
26. Abbott SB, Stornetta RL, Coates MB, Guyenet PG. Phox2b-expressing neurons of the parafacial region regulate breathing rate, inspiration, and expiration in conscious rats. J Neurosci **2011**; 31:16410–22.
27. Kanbar R, Stornetta RL, Cash DR, Lewis SJ, Guyenet PG. Photostimulation of Phox2b medullary neurons activates cardiorespiratory function in conscious rats. Am J Respirat Crit Care Med **2010**; 182:1184–94.
28. Gonzalez-Forero D, Portillo F, Gomez L, Montero F, Kasparov S, Moreno-Lopez B. Inhibition of resting potassium conductances by long-term activation of the NO/cGMP/protein kinase G pathway: a new mechanism regulating neuronal excitability. J Neurosci **2007**; 27:6302–12.
29. Webster RG, Brain KL, Wilson RH, Grem JL, Vincent A. Oxaliplatin induces hyperexcitability at motor and autonomic neuromuscular junctions through effects on voltage-gated sodium channels. Br J Pharmacol **2005**; 146:1027–39.
30. Young JK, Wu M, Manaye KF, et al. Orexin stimulates breathing via medullary and spinal pathways. J Appl Physiol **2005**; 98:1387–95.
31. Hervieu GJ, Cluderay JE, Harrison DC, Roberts JC, Leslie RA. Gene expression and protein distribution of the orexin-1 receptor in the rat brain and spinal cord. Neuroscience **2001**; 103:777–97.
32. Llona I, Eugenin J. Central actions of somatostatin in the generation and control of breathing. Biol Res **2005**; 38:347–52.
33. Dubreuil V, Thoby-Brisson M, Rallu M, et al. Defective respiratory rhythmogenesis and loss of central chemosensitivity in Phox2b mutants targeting retrotrapezoid nucleus neurons. J Neurosci **2009**; 29: 14836–46.
34. Smeraski CA, Siddharthan V, Morrey JD. Treatment of spatial memory impairment in hamsters infected with West Nile virus using a humanized monoclonal antibody MGAWN1. Antiviral Research **2011**; 91:43–9.
35. Sejvar JJ, Bode AV, Marfin AA, et al. West Nile virus-associated flaccid paralysis. Emerg Infect Dis **2005**; 11:1021–7.
36. Sejvar JJ, Bode AV, Marfin AA, et al. West Nile Virus-associated flaccid paralysis outcome. Emerg Infect Dis **2006**; 12:514–6.
37. Fratkin JD, Leis AA, Stokic DS, Slavinski SA, Geiss RW. Spinal cord neuropathology in human West Nile virus infection. Arch Pathol Lab Med **2004**; 128:533–7.
38. Cao NJ, Ranganathan C, Kupsky WJ, Li J. Recovery and prognosticators of paralysis in West Nile virus infection. J Neurol Sci **2005**; 236:73–80.
39. Hase T, Dubois DR, Summers PL, Downs MB, Ussery MA. Comparison of replication rates and pathogenicities between the SA14 parent and SA14–14-2 vaccine strains of Japanese encephalitis virus in mouse brain neurons. Arch Virol **1993**; 130:131–43.
40. Isachkova LM, Shestopalova NM, Frolova MP, Reingold VN. Light and electron microscope study of the neurotropism of Powassan virus strain P-40. Acta Virol **1979**; 23:40–4.
41. Tavakoli NP, Wang H, Dupuis M, et al. Fatal case of deer tick virus encephalitis. N Engl J Med **2009**; 360:2099–107.
42. Schoneboom BA, Fultz MJ, Miller TH, McKinney LC, Grieder FB. Astrocytes as targets for Venezuelan equine encephalitis virus infection. J Neurovirol **1999**; 5:342–54.
43. Steele KE, Twenhafel NA. Pathology of animal models of alphavirus encephalitis. Vet Pathol **2010**; 47:790–805.
44. Fernandez-Espejo E. Pathogenesis of Parkinson's disease: prospects of neuroprotective and restorative therapies. Mol Neurobiol **2004**; 29: 15–30.
45. Nihei K, McKee AC, Kowall NW. Patterns of neuronal degeneration in the motor cortex of amyotrophic lateral sclerosis patients. Acta Neuropathol **1993**; 86:55–64.